


Structure and Phase Transformations in Thin Films

Zsolt Czirány 

Centre for Energy Research, Institute of Technical Physics and Materials Science, Konkoly Thege M. út 29-33,
H-1121 Budapest, Hungary; czirany.zsolt@ek-cer.hu

1. Introduction

The field of thin films has gone through a great development in recent decades. Besides the multiple applications of thin films, an increasing competence can be observed in tailoring the film microstructure via composition and deposition parameters. The first approach led to the development of, e.g., multicomponent carbide, nitride and oxynitride [1,2] hard coatings and superalloys [3,4], and turned recent interest towards high-entropy alloys [5–8]. The latter approach resulted in significant improvement of deposition techniques where energetic surface bombardment can influence surface mobility and the formed bonding at the growth surface [9,10]. Revealing the microstructure is inevitable for understanding how defects, the ordering of atoms within the crystalline unit cell or the formation of multiple phases and their arrangement influences the performance of coatings on the macroscopic scale. Structural features on the nanoscale may also provide excellent properties to novel nanocomposites and special nanolaminated structures, e.g., MAX phases [11–13]. The achievements that can be quantified in terms of hardness, elasticity, corrosion resistance or adhesion can be utilized in the improved lifetime of coatings and coated parts. However, we know little about the effect of additives and their role in the secondary phase formation and segregation and their influence on macroscopic properties (e.g., corrosion). Moreover, the research is often limited to the formed phases and structures. The existing knowledge should be completed with the exploration of the mechanism of the ongoing processes by their in situ monitoring. The recent development of state-of-the-art in situ TEM specimen holders may boost the available information about the structural transformations due to an elevated temperature, deformation or chemical ambient.

2. Review of Special Issue Contents

This Special Issue [14–23] aimed at attracting cutting-edge research and review articles on the preparation and characterization of materials with excellent properties or the related modelling approaches. The published papers in this Special Issue cover a wide range of topics, including high-entropy alloys [14], hard materials [15,21,23], effects of additives [15,17,18] on structure and properties, and the identification of Magnéli phases [22]. Computer modelling of magnetic properties [19,20] and optical modelling of dielectric function [16] are also represented in this volume.

The first published paper [14] presents an in situ TEM-annealing study of the microstructural evolution of CrFeCoNiCu high-entropy alloy (HEA) thin films. A post-annealing investigation of the samples was carried out using high-resolution transmission electron microscopy and EDS measurements. The film is a structurally stable single-phase FCC HEA up to 400 °C. At 450 °C, the formation of a BCC phase was observed; however, the morphology of the film was preserved. This type of transformation is attributed to diffusionless processes (martensitic or massive), while the fast morphological and structural changes above 550 °C are controlled by volume diffusion processes. The structure of the intermetallic phase formed at high temperatures is modelled as a supercell of the BCC phase.

The second paper [15] shows an example of how additives can influence the mechanical properties of a material. They studied the influence of 0.4–5.3 at% Mo addition on



Citation: Czirány, Z. Structure and Phase Transformations in Thin Films.

Coatings **2023**, *13*, 1233. <https://doi.org/10.3390/coatings13071233>

Received: 12 June 2023

Revised: 27 June 2023

Accepted: 5 July 2023

Published: 11 July 2023



Copyright: © 2023 by the author. Licensee MDPI, Basel, Switzerland. This article is an open access article distributed under the terms and conditions of the Creative Commons Attribution (CC BY) license (<https://creativecommons.org/licenses/by/4.0/>).

the compression behaviour of electrodeposited Ni films using micropillar deformation tests. They observed a lower grain size and higher dislocation and twin density at high Mo content, the differences of which resulted in a four-times higher yield strength compared to low Mo samples. The strain softening of low Mo samples after repeated deformation was attributed to detwinning during deformation.

In the third paper [16], amorphous Ge (a-Ge) was created in single-crystalline Ge via ion implantation. It was shown that high optical density is available when implanting low-mass Al ions using a dual-energy approach. The optical properties were measured using multiple angle of incidence spectroscopic ellipsometry. The Cody–Lorentz dispersion model was the most suitable and was capable of describing the dielectric function using a few parameters in the wavelength range from 210 to 1690 nm. The results of the optical model were consistent with Rutherford backscattering spectrometry and cross-sectional electron microscopy measurements, including the agreement of the layer thickness within experimental uncertainty. Accurate reference dielectric functions play an important role in the research development and reproducible preparation of optical materials, such as in integrated optics, optoelectronics or photovoltaics.

In the fourth paper [17], the effect of (~28 and 32 at%) N incorporation was investigated using X-ray diffraction on nitrogen-containing 304 stainless steel thin films deposited by reactive RF magnetron sputtering as a function of substrate temperature and bias. The extent of the diffraction anomaly, i.e., relative peak shifts of (111) and (200) peak positions, was determined using a calculated parameter, denoted $R_B = \sin^2\theta_{111}/\sin^2\theta_{200}$. The normal value for R_B for FCC-based structures is 0.75, and R_B increases as the (002) peak shifts closer to the (111) peak. In this study, the R_B values for the deposited films increased with substrate bias but decreased with substrate temperature (but still always >0.75). Since the split of 200 reflection (due to assumed tetragonal distortion) was not observed, a defect-based hypothesis is more viable as an explanation for the diffraction anomaly.

In the fifth paper [18], amorphous hydrogen-free silicon nitride (a-SiN_x) and amorphous hydrogenated silicon nitride (a-SiN_x:H) films were deposited via radio frequency (RF) sputtering applying various hydrogen flows. The refractive index of 1.96 was characteristic for hydrogen-free SiN_x thin film, and with increasing H₂ flow, it decreased to 1.89. Hydrogenation during the sputtering process increased the porosity of the thin films compared with hydrogen-free SiN_x. Higher porosity is consistent with a lower refractive index. The hydrogen content of hydrogenated films was 4 at% and 6 at% according to Fourier-transform infrared spectroscopy (FTIR) and elastic recoil detection analysis (ERDA), respectively. The molecular form of hydrogen was released at a temperature of ~65 °C from the film after annealing, while blisters of 100 nm in diameter were formed on the thin film surface. The low activation energy deduced from the Arrhenius method indicated the diffusion of hydrogen molecules.

The sixth paper [19] provides a study of the Néel phase transition temperature of Fe₂O₃ nanocomposite thin films via Monte-Carlo simulation taking into account a variety of parameters. They found that particle size and magnetic field are the main parameters that determine the temperature of Néel transition (T_{Ntot}). The results also show that in Fe₂O₃ thin films, T_{Ntot} is always smaller than in the case of Fe₂O₃ nanoparticles and bulk Fe₂O₃. For a nanoparticle size of 12 nm, $T_{Ntot} = 300$ K. Furthermore, there is a linear relationship between T_{Ntot} and nanoparticle size. The results can be utilized in the design of magnetic devices and in biomedical applications.

The seventh paper [20] is another computer simulation modelling of the ferroelectric substrate influence on the condition and magnetic properties of 2D ferromagnetic nanofilms using the two-dimensional Frenkel–Kontorova (FK) potential to simulate the substrate effect on the film. The Ising model and Wolf cluster algorithm are used to describe the magnetic behaviour of an FM film. The results show that uniform deformations of the substrate lead to inhomogeneous deformations of the film. The interaction between the substrate and film causes film deformations leading to superstructures with low and high atomic concentrations. Heating or external electric field can cause substrate deformations,

and consequent substrate-induced structural phase transition takes place. The Curie temperature decreases with both substrate compression and stretching.

In the eighth paper [21], the properties of $\text{Ti}_x\text{Zr}_{1-x}\text{N}$ hard coatings were investigated. $\text{Ti}_x\text{Zr}_{1-x}\text{N}$ films with $\text{Zr}/(\text{Zr} + \text{Ti})$ molar ratios from 20% to 80% were prepared with multi-arc ion plating using different combinations of either elemental Ti and Zr or TiZr alloy targets. The as-deposited $\text{Ti}_x\text{Zr}_{1-x}\text{N}$ films formed substitutional fcc solid solutions with a lattice constant consistent with Vegard's law. When the Zr/Ti molar ratio was 40:60 or 60:40, the films showed (111) and (220) preferred growth orientation, while at other compositions, the films exhibited (111) preferred orientation. These two compositions coincide with the hardness maxima with values over 30 GPa.

In the ninth paper [22], the structure and phase transition of V_4O_7 Magnéli phase was investigated. A thin film of vanadium oxide Magnéli phase V_4O_7 was produced using cathodic arc sputtering of V target at 600 °C and 0.045 Pa of oxygen atmosphere. The stoichiometric composition of V_4O_7 was confirmed using Rutherford backscatter spectrometry. The similarity of structures of Magnéli phases may make it challenging to identify the phase precisely using X-ray diffraction, especially if the sample is nanostructured, highly textured, and strained. The authors proved that Raman spectroscopy can be a sensitive indicator of minor structural changes even at room temperature with the careful tuning of the laser power on the sample. Metal–insulator phase transition in V_4O_7 thin films was observed via Raman spectroscopy between −50 and −55 °C.

In the tenth paper [23], the composition of AlCrTiN quaternary nitride films is optimized. Ternary nitrides, like TiCrN, generally form face-centred cubic solid solutions and have superior properties in terms of phase composition, hardness, and thermal shock resistance and adhesion to the substrate due to the addition of alloying elements. The effect of high Al content was investigated in this work. AlCrTiN hard coatings were prepared via reactive multi-arc ion plating on high-speed steel substrates via the co-deposition of AlCr and AlTi dual-arc source alloy targets in N. The optimal composition of the AlCrTiN hard films is 25:13:15:47 (at%), based on the consideration of hardness, adhesion, and thermal shock cycling resistance. This optimal AlCrTiN hard film can be suggested as an option for protective coatings in applications up to 600 °C.

Funding: National Research Development and Innovation Fund Office, Hungary, Grant Number: K-125100.

Conflicts of Interest: The author declares no conflict of interest.

References

1. Gogotsi, Y.G.; Andrievski, R.A. (Eds.) *Materials Science of Carbides, Nitrides and Borides in NATO Science Series, 3 High Technology—Volume 68*; Springer-Science+Business Media: Dordrecht, The Netherlands, 1999.
2. Rasaki, S.A.; Zhang, B.; Anbalgam, K.; Thomas, T.; Yang, M. Synthesis and application of nano-structured metal nitrides and carbides: A review. *Prog. Solid State Chem.* **2018**, *50*, 1–15. [CrossRef]
3. Moverare, J. (Ed.) Special Issue “Superalloys”. Available online: https://www.mdpi.com/journal/metals/special_issues/superalloys (accessed on 4 July 2023).
4. Shahwaz, M.; Nath, P.; Sen, I. A critical review on the microstructure and mechanical properties correlation of additively manufactured nickel-based superalloys. *J. Alloys Compd.* **2022**, *907*, 164530. [CrossRef]
5. Cantor, B.; Chang, I.T.H.; Knight, P.; Vincent, A.J.B. Microstructural development in equiatomic multicomponent alloys. *Mater. Sci. Eng. A* **2004**, *375*, 213–218. [CrossRef]
6. Miracle, D.B.; Senkov, O.N. A critical review of high entropy alloys and related concepts. *Acta Mater.* **2017**, *122*, 448–511. [CrossRef]
7. George, E.P.; Curtin, W.A.; Tasan, C.C. High entropy alloys: A focused review of mechanical properties and deformation mechanisms. *Acta Mater.* **2020**, *188*, 435–474. [CrossRef]
8. Kumari, P.; Gupta, A.K.; Mishra, R.K.; Ahmad, M.S.; Shahi, R.R. A Comprehensive Review: Recent Progress on Magnetic High Entropy Alloys and Oxides. *J. Magn. Magn. Mater.* **2022**, *554*, 169142. [CrossRef]
9. Mattox, D.M. Particle bombardment effects on thin-film deposition: A review. *J. Vac. Sci. Technol. A* **1989**, *7*, 1105–1114. [CrossRef]
10. Aghda, S.K.; Holzapfel, D.M.; Music, D.; Unutulmazsoy, Y.; Mráz, S.; Bogdanovski, D.; Fidanboy, G.; Hans, M.; Primetzhofer, D.; Méndez, A.S.J.; et al. Ion kinetic energy- and ion flux-dependent mechanical properties and thermal stability of (Ti,Al)N thin films. *Acta Mater.* **2023**, *250*, 118864. [CrossRef]

11. Barsoum, M.W.; El-Raghy, T. The MAX Phases: Unique New Carbide and Nitride Materials: Ternary ceramics turn out to be surprisingly soft and machinable, yet also heat-tolerant, strong and lightweight. *Am. Sci.* **2001**, *89*, 334–343. [\[CrossRef\]](#)
12. Barsoum, M.W.; Radovic, M. Elastic and Mechanical Properties of the MAX Phases. *Annu. Rev. Mater. Res.* **2011**, *41*, 195–227. [\[CrossRef\]](#)
13. Lei, X.; Lin, N. Structure and synthesis of MAX phase materials: A brief review. *Crit. Rev. Solid State Mater. Sci.* **2022**, *47*, 736–771. [\[CrossRef\]](#)
14. Arfaoui, M.; Radnóczy, G.; Kis, V.K. Transformations in CrFeCoNiCu High Entropy Alloy Thin Films during In-Situ Annealing in TEM. *Coatings* **2020**, *10*, 60. [\[CrossRef\]](#)
15. Gubicza, J.; Kapoor, G.; Ugi, D.; Péter, L.; Lábár, J.L.; Radnóczy, G. Micropillar Compression Study on the Deformation Behavior of Electrodeposited Ni–Mo Films. *Coatings* **2020**, *10*, 205. [\[CrossRef\]](#)
16. Lohner, T.; Szilágyi, E.; Zolnai, Z.; Németh, A.; Fogarassy, Z.; Illés, L.; Kótai, E.; Petrik, P.; Fried, M. Determination of the Complex Dielectric Function of Ion-Implanted Amorphous Germanium by Spectroscopic Ellipsometry. *Coatings* **2020**, *10*, 480. [\[CrossRef\]](#)
17. Alresheedi, F.I.; Krzanowski, J.E. X-ray Diffraction Investigation of Stainless Steel-Nitrogen Thin Films Deposited Using Reactive Sputter Deposition. *Coatings* **2020**, *10*, 984. [\[CrossRef\]](#)
18. Hegedüs, N.; Lovics, R.; Serényi, M.; Zolnai, Z.; Petrik, P.; Mihály, J.; Fogarassy, Z.; Balázs, C.; Balázs, K. Examination of the Hydrogen Incorporation into Radio Frequency-Sputtered Hydrogenated SiNx Thin Films. *Coatings* **2021**, *11*, 54. [\[CrossRef\]](#)
19. Trong, D.N.; Long, V.C.; Talu, S. The Study of the Influence of Matrix, Size, Rotation Angle, and Magnetic Field on the Isothermal Entropy, and the Néel Phase Transition Temperature of Fe₂O₃ Nanocomposite Thin Films by the Monte-Carlo Simulation Method. *Coatings* **2021**, *11*, 1209. [\[CrossRef\]](#)
20. Bychkov, I.; Belim, S.; Maltsev, I.; Shavrov, V. Phase Transition and Magnetoelectric Effect in 2D Ferromagnetic Films on a Ferroelectric Substrate. *Coatings* **2021**, *11*, 1325. [\[CrossRef\]](#)
21. Zhang, J.; Peng, L.; Wang, X.; Liu, D.; Wang, N. Effects of Zr/(Zr+Ti) Molar Ratio on the Phase Structure and Hardness of Ti_xZr_{1-x}N Films. *Coatings* **2021**, *11*, 1342. [\[CrossRef\]](#)
22. Shvets, P.; Maksimova, K.; Goikhman, A. Raman Spectroscopy of V₄O₇ Films. *Coatings* **2022**, *12*, 291. [\[CrossRef\]](#)
23. Peng, L.; Zhang, J.; Wang, X. Phase Composition, Hardness, and Thermal Shock Properties of AlCrTiN Hard Films with High Aluminum Content. *Coatings* **2023**, *13*, 547. [\[CrossRef\]](#)

Disclaimer/Publisher's Note: The statements, opinions and data contained in all publications are solely those of the individual author(s) and contributor(s) and not of MDPI and/or the editor(s). MDPI and/or the editor(s) disclaim responsibility for any injury to people or property resulting from any ideas, methods, instructions or products referred to in the content.